COMMENTS AND OPINIONS

Journal of Semiconductors
(2021) 42, 080301
doi: 10.1088/1674-4926/42/8/080301

All-polymer solar cells

Baoqi Wu[1, ‡], Bingyan Yin[1, ‡], Chunhui Duan[1, †], and Liming Ding[2, †]

[1]State Key Laboratory of Luminescent Materials and Devices, South China University of Technology, Guangzhou 510640, China

[2]Center for Excellence in Nanoscience (CAS), Key Laboratory of Nanosystem and Hierarchical Fabrication (CAS), National Center for Nanoscience and Technology, Beijing 100190, China

Citation: B Q Wu, B Y Yin, C H Duan, and L M Ding, All-polymer solar cells[J]. *J. Semicond.*, 2021, 42(8), 080301. http://doi.org/10.1088/1674-4926/42/8/080301

Organic solar cells (OSCs) show a promising commercialization prospect with their power conversion efficiencies (PCEs) exceeding 18%[1–6]. Among various types of OSCs, all-polymer solar cells (all-PSCs) with a physical blend of p- and n-type polymer as the active layer to harvest solar irradiation attract growing attention due to their unique advantages like excellent morphological stability, and mechanical durability[7]. Recently, great progresses have been achieved in this field including the development of high-performance polymer acceptors and the advances in morphology regulation[8–13]. Particularly, a PCE of 17.20% has been realized very recently by all-PSCs *via* properly aligned energy levels and optimal active-layer morphology[8]. This achievement has significantly reduced the PCE gap between all-PSCs and small molecular acceptor-based OSCs, indicating the bright future of all-PSCs. Therefore, a highlight on these important progresses is timely and will effectively drive the development of all-PSCs.

In the early stage, the electron acceptors employed in all-PSCs were mainly dominated by perylene diimide (PDI) and naphthalene diimide (NDI) polymers[7, 14–18]. Specifically, an NDI-based polymer with a trade name of N2200 (Fig. 1) is the most widely used electron acceptor in all-PSCs[19–22]. This polymer was initially reported by Facchetti *et al.* in 2009, which exhibited appropriate lowest unoccupied molecular orbital (LUMO) energy level (~–4.0 eV) and high electron mobility (~10^{-3} $cm^2/(V{\cdot}s)$)[23]. Through delicate optimization of the active-layer morphology, the highest PCE of all-PSCs with N2200 reached 11.76%, which is comparable to that of fullerene-based OSCs[22]. However, further efficiency improvement of N2200-based all-PSCs was hampered by the limited short-circuit current density (J_{sc}). This is caused by the low external quantum efficiency (EQE) in the long wavelength region due to the low absorption coefficient (~3×10^4 cm^{-1} at 700 nm) of N2200. Besides, NDI-based polymers usually lead to the formation of large domains in active layer due to the strong aggregation ability of NDI-based polymers. Considerable efforts were thus devoted to regulate the morphology of the active layer of all-PSCs with NDI polymers. The reported morphology optimization strategies span from chemistry (such as side chain functionalization, co-monomer selection, ternary copolymerization, etc.)[24–27] to physics (such as the selection of matched donors, solvent optimization, post-treatment by thermal annealing or solvent annealing, etc.)[28–31]. An important advantage of NDI-based polymers is that they can afford very stable devices[32–34], which makes them a class of promising polymer acceptors should the device efficiency can be further improved.

To overcome the drawbacks associated with NDI- and PDI-based polymers, a few n-type polymers with donor–acceptor alternating skeleton were thus developed for use as electron acceptors in all-PSCs[35–39]. In 2015, Liu and co-workers reported a polymer acceptor featuring boron-nitrogen coordination bond (B←N) for all-PSCs[35], which offered high open-circuit voltage (V_{oc}) due to the high-lying LUMO energy level. After that, a few polymer acceptors based on B←N coordination bond with superior optoelectronic properties were developed[40]. For example, PBN-12 (Fig. 1) afforded a decent PCE of 10.1% and a high V_{oc} of 1.17 V benefitting from the high LUMO level of the polymer[37]. However, this polymer suffered from narrow light absorption range due to the large optical bandgap of 1.78 eV. As a result, the J_{sc} of the best all-PSCs with PBN-12 only reached 13.39 mA/cm^2. Guo group developed a donor–acceptor alternating narrow-bandgap polymer acceptor (DCNBT-IDT, Fig. 1) based on the electron-deficient unit 5,6-dicyano-2,1,3-benzothiadiazole (DCNBT), possessing an optical bandgap of 1.43 eV[38]. The all-PSCs with DCNBT-IDT offered a decent PCE of 8.32% when blended with the polymer donor PBDB-T. By copolymerizing DCNBT with a stronger electron-rich monomer, the resulting polymer DCNBT-TPIC (Fig. 1) further extended the light absorption onset to 970 nm and obtained a maximum absorption coefficient of ~7.5×10^4 cm^{-1}[39]. As a result, the best all-PSC with DCNBT-TPIC gave a PCE of 10.22% with a J_{sc} of 22.52 mA/cm^2. However, the fill factor (FF) of all-PSCs with DCNBT-IDT or DCNBT-TPIC was ~0.65, which restricted the overall device performance. Encouragingly, an FF of 0.74 was achieved by DCNBT-IDT *via* a delicate design of ternary blend and p-doping the polymer donor with 2,3,5,6-tetrafluoro-7,7,8,8-tetracyanoquinodimethane (F4-TCNQ), yielding a remarkable PCE of 11.87%[41]. These results demonstrated the potential of DCNBT-based polymers for high-performance all-PSCs.

The leap-forward advance of all-PSCs should be attributed to the strategy of the polymerization of non-fullerene small molecular acceptors (Fig. 1)[42, 43]. This kind of polymers (PSMAs) retain the merits of their parent small molecular acceptors including narrow optical bandgap, high light absorption coefficient, suitable energy levels, and high charge mobility[44]. This strategy was first reported by Li group in 2017 with the synthesis of PZ1 (Fig. 1), which is a polymer of A–D–A type small molecular acceptor IDIC[42, 45]. Impressively,

Baoqi Wu and Bingyan Yin contributed equally to this work.

Correspondence to: C H Duan, duanchunhui@scut.edu.cn; L M Ding, ding@nanoctr.cn

Received 19 JUNE 2021.

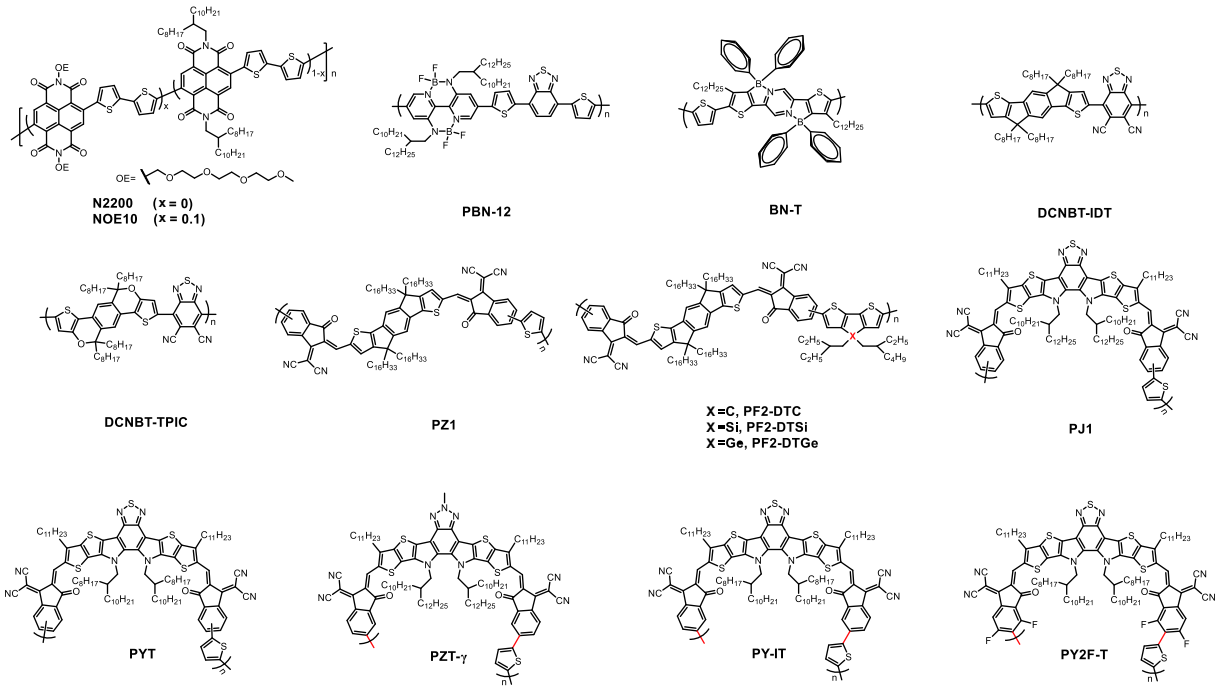

Fig. 1. Chemical structures of the polymer acceptors.

Table 1. Performance data for all-PSCs.

Acceptor	Donor	V_{oc} (V)	J_{sc} (mA/cm^2)	FF	PCE (%)	Ref.
N2200	PTzBI-Si	0.88	17.6	0.76	11.76	[22]
NOE10	PBDT-TAZ	0.84	12.9	0.75	8.10	[34]
PBN-12	CD1	1.17	13.4	0.64	10.07	[37]
DCNBT-TPIC	PBDTTT-E-T	0.70	22.5	0.65	10.22	[39]
DCNBT-IDT	PBDB-T/ PNDT-T	0.91	17.5	0.74	11.87	[41]
PZ1	PM6	0.96	17.1	0.68	11.20	[45]
PJ1	JD40	0.91	23.2	0.75	15.80	[11]
PYT	PBDB-T	0.89	23.0	0.74	15.17	[54]
PZT-γ	PBDB-T	0.90	24.7	0.71	15.80	[12]
PY-IT/BNT	PM6	0.96	22.7	0.74	16.09	[9]
PY2F-T/PYT	PM6	0.90	25.2	0.76	17.20	[8]

a highly efficient all-PSC with a PCE of 9.19% was made based on PZ1. This result greatly stimulated the activities in developing high-performance polymer acceptors by polymerizing non-fullerene small molecular acceptors. More recently, several polymer acceptors based on a prevailing small molecular acceptor, Y6, were synthesized by several groups[43, 46–51]. For example, the polymer PJ1 (Fig. 1) developed by Huang group afforded a PCE of 14.4%, which is the record efficiency for all-PSCs at that time[43]. Further, a higher PCE of 15.4% and an FF over 0.75 were achieved through tuning the molecular weights of the polymer donor (PBDB-T) to form optimal active-layer morphology[52]. One of the drawbacks of this kind of polymer acceptors is the large batch-to-batch variation. Taking PYT (Fig. 1) as an example, the PCEs for all-PSCs with PYT made by different groups varied from 11% to 15%[47, 51, 53, 54]. This issue might be caused by the fact that the polymers are isomeric mixtures due to the position of the terminal Br atom is uncertain. Further efforts were thus devoted to synthesizing polymer acceptors with isomerically pure monomers. These polymers offered over 15% efficiency in the resulting all-PSCs, which evidenced the significance of regioregularity control of this kind of polymers[8, 9, 12, 55, 56]. For example, Jen group[12] reported a regioregular polymer acceptor PZT-γ (Fig. 1) based on Y6, which gave an impressive PCE of 15.8% with a high J_{sc} of 24.7 mA/cm^2. Under the same condition, the reference polymer PZT with irregular conjugated main chain offered a lower PCE of 14.5%. Another issue associated with this kind of polymers lies in the chemical and photo-oxidation instability, which has been widely recognized in their parent small molecular acceptors[57–60]. Therefore, further evaluation is needed before the practical application of this kind of polymers.

Morphology optimization for the active layer is another key for realizing high-performance all-PSCs. In most cases, excessive phase separation occurred due to the reduced entropic contribution in all-polymer blends, which thereby resulted in limited donor/acceptor interfaces and small J_{sc}[61]. Besides, intimately mixed morphology can also be formed when the polymer donor and acceptor are too miscible, which in turn hampers charge transport and leads to severe geminate and nongeminate recombination[7]. Generally, the active-layer morphology of all-PSCs can be optimized by controlling the film deposition process and performing post-treatment. For example, Zhu *et al.*[22] found that the use of a volatile solvent, 2-methyltetrahydrofuran (MTHF), can freeze the morphology of the blend of PTzBI-Si (Fig. 2) and N2200 at the early stage of phase separation and maintain a moderate crystalline fibril network, whereas the blend film processed from a high boiling-point solvent, chlorobenzene (CB), showed excessive phase separation with large domains (Fig. 3). The film crystallinity was further improved by subsequent thermal and solvent vapor annealing, which effectively facilitated charge transport and reduced the recombination. As a result, the all-PSC processed from MTHF gave a PCE of 11.76%, which is five times higher than that for the device processed from CB.

Ternary blend strategy is frequently used to optimize the active-layer morphology of all-PSCs. For example, the in-

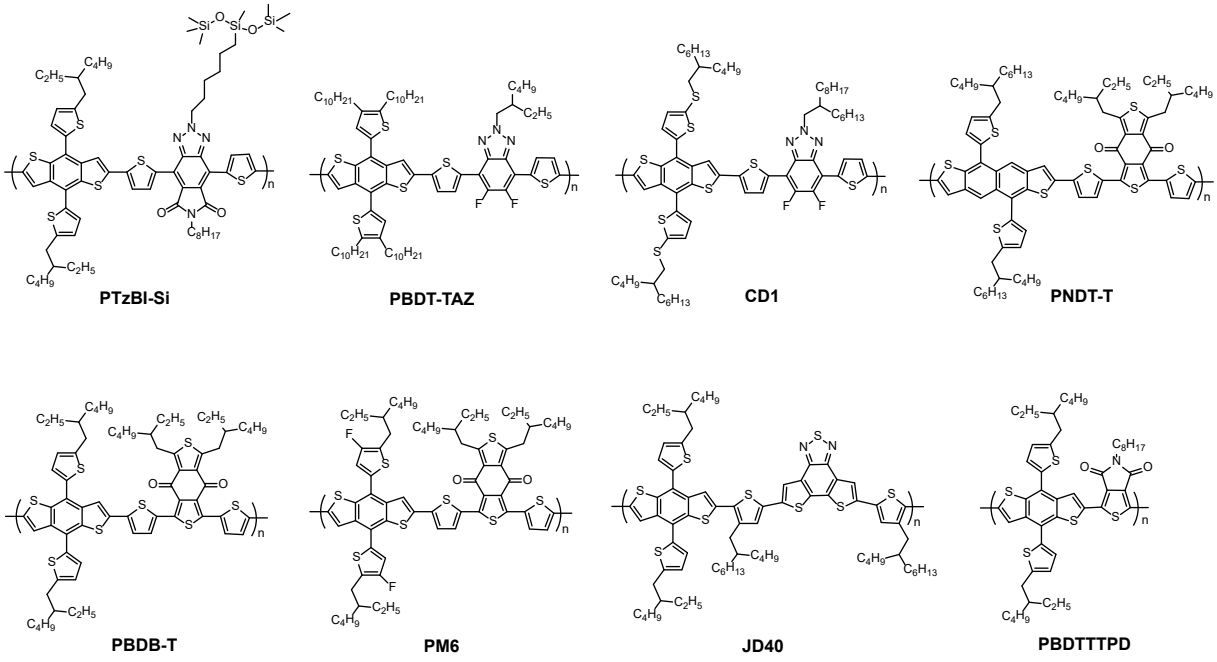

Fig. 2. Chemical structures of the polymer donors.

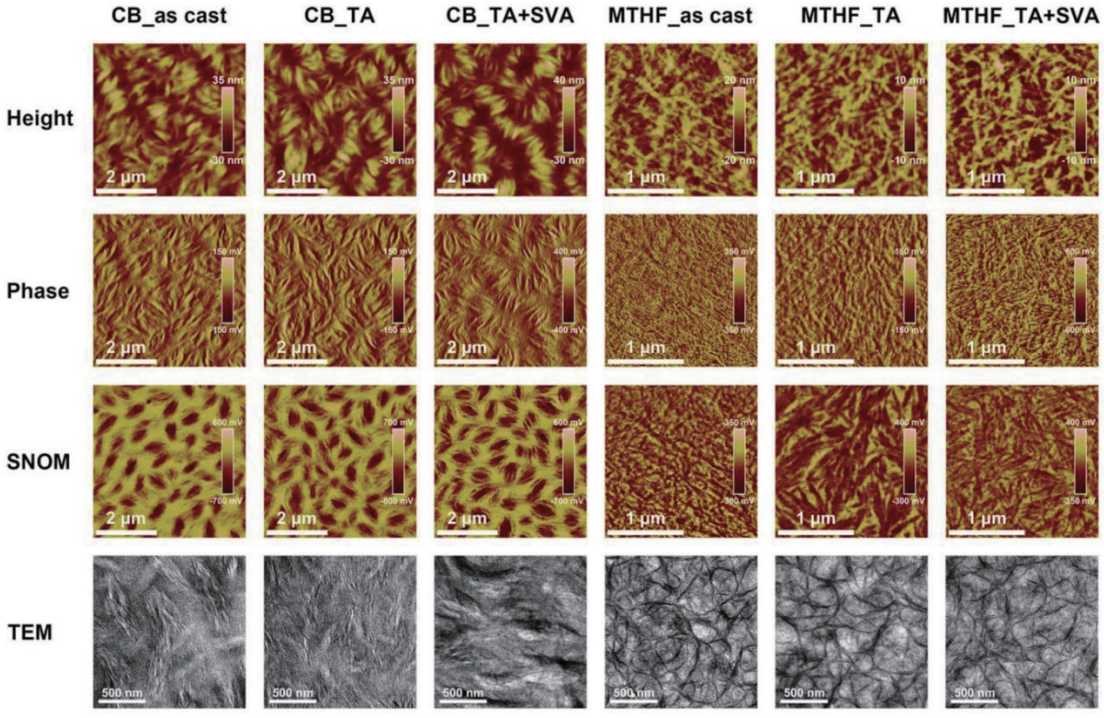

Fig. 3. (Color online) Atomic force microscopy (AFM) height (first row) and phase (second row) images, scanning near-field optical microscopy (SNOM) images (third row), and transmission electron microscopy (TEM) images (fourth row) for PTzBI-Si:N2200 blend films processed under different conditions. Reproduced with permission[22], Copyright 2019, John Wiley and Sons.

creased crystallinity of the host polymer acceptor (PY-IT) with more compact lamellar and π–π stacking has been achieved by introducing the third component BN-T (Fig. 1) into the PM6:PY-IT blend, which is beneficial to exciton splitting and charge transport[9]. Meanwhile, the scale of phase separation was not influenced. As a result, the ternary all-PSCs based on PM6:PY-IT:BN-T achieved a remarkable PCE of 16.09%, which is considerably higher than the PCE (15.11%) given by PM6:PY-IT cells. More recently, Sun *et al.* demonstrated that the addition of PYT could reduce the π–π stacking distance and maintain a favorable face-on orientation of the polymer acceptor in PM6:PYT:PY2F-T blend without negatively affecting the phase separation. The PM6:PYT:PY2F-T cells gave a PCE of 17.20%, significantly outperforming the PM6:PYT (14.5%) and PM6:PY2F-T cells (15.0%)[8].

The formation of pseudo-bilayer structure or P–i–N structure *via* layer-by-layer deposition of polymer donor and acceptor is effective to modulate the active layer morphology of all-PSCs, which can avoid the complicated phase separation process in bulk-heterojunction (BHJ) blend and simplify morpho-

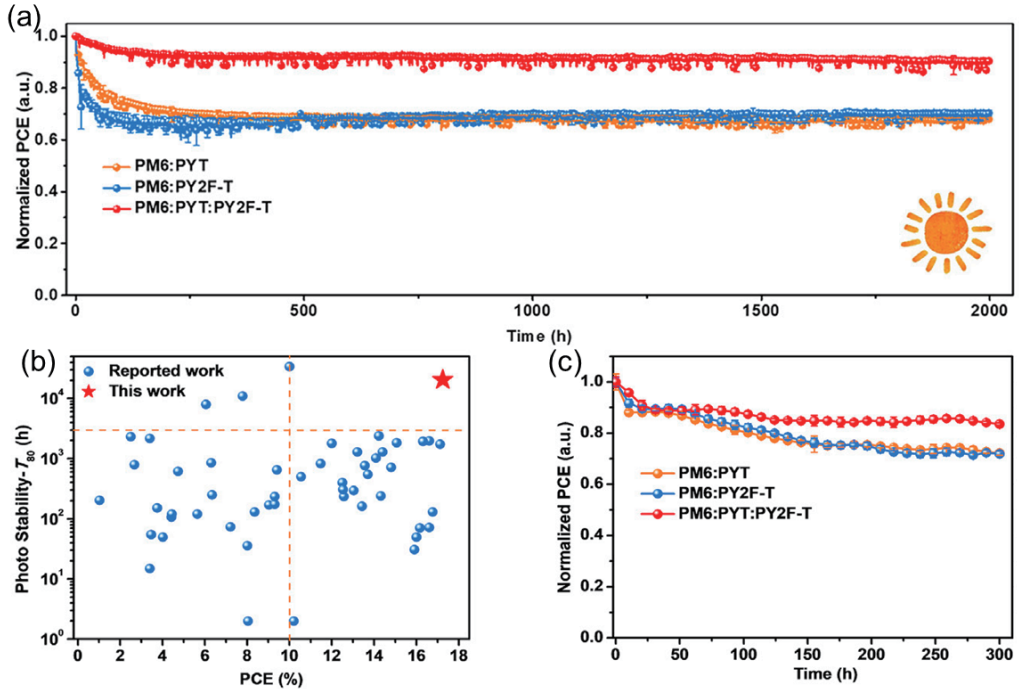

Fig. 4. (Color online) (a) Normalized PCEs as a function of light-soaking time. (b) The performance versus T_{80} lifetimes of PSCs reported so far. (c) Normalized PCEs for the devices under continuous illumination in a nitrogen glovebox at 65 °C. Reproduced with permission[8], Copyright 2021, Elsevier.

logy control. Besides, the pseudo-bilayer configuration can offer desirable vertical gradient distribution in the active layer. Pioneering work of pseudo-bilayer all-PSCs was performed by Xu *et al.*[62], in which PBDB-T and N2200 were used as the polymer donor and acceptor, respectively. Both the donor and acceptor layers are highly ordered with a face-on orientation, which enabled more efficient charge separation, better carrier transport, and less trap-assisted recombination in comparison to the BHJ device. As a result, a PCE of 9.52% was achieved, nearly 50% improvement compared with the BHJ device. Based on the same strategy, Wu *et al.*[54] achieved a remarkable PCE of 15.2% in PBDB-T/PYT pseudo-bilayer device. These results proved that layer-by-layer deposition is a practically useful method to achieve high-performance all-PSCs.

Device stability is of great importance for commercial applications[63]. Liu *et al.*[34] compared the stability of PSCs based on the same polymer donor (PBDT-TAZ) and different acceptors (PCBM, ITIC, and NOE10) (Figs. 1 and 2). The all-PSC of PBDT-TAZ:NOE10 exhibited greatly improved stability compared with other devices, whose PCE retained 95% after 400 h of storage in a nitrogen-filled glovebox at room temperature under dark. Under the same conditions, the PCBM- and ITIC-based solar cells retained less than 70% of their initial PCE after 100 h. Moreover, the all-PSC of PBDT-TAZ:NOE10 showed superior thermal stability with >97% of its initial PCE after 300 h continuous thermal aging at 65 °C. All-PSCs were also reported to be stable under continuous light illumination. The PM6:PY2F-T:PYT ternary cells were exposed to constant light illumination under both room and elevated temperature[8]. Impressively, only a slight decrease in PCE was observed after 200 h simulated 1-sun illumination. Subsequently, the PCE reached an almost steady state and maintained 90.5% of its initial PCE after continuous illumination for 2000 h at room temperature. The extrapolated time for retaining 80% initial efficiency (T_{80}) is up to 20 500 h (Figs. 4(a) and 4(b)). More importantly, the PM6:PY2F-T:PYT cells retained 83.5% of their initial PCE under continuous illumination and thermal aging at 65 °C in a nitrogen-filled glovebox (Fig. 4(c)). These results demonstrate that all-PSCs can operate stably under synergistic light and thermal stresses.

Another important merit of all-PSCs is their mechanical flexibility. The great tolerance to severe mechanical deformation of all-PSCs provides an advantage for application in flexible and stretchable devices. Kim *et al.*[64] took the lead to fabricate flexible all-PSCs. The all-PSCs of PBDTTTPD:N2200 (Fig. 2) exhibited ductile crack grow in contrast with obvious brittle crack propagation of fullerene-based solar cells, leading to 60- and 470-fold improvement in elongation at break and toughness, respectively. Yang *et al.*[65] used a sticky polymer (PDPS) as additive to reinforce the toughness of N2200-based all-PSCs (Fig. 5(a)). Adding 10 wt% PDPS into the polymer matrix, the resulting film exhibited superior toughness up to 9.67 MJ/m^3 with an elongation at break of 50.92%, and the blend film deposited on polyethylene terephthalate (PET) can twist (Figs. 5(b)–5(d)). The device maintained 90% of the initial PCE after 100 bending cycles with a bending radius of 3.0 mm (Fig. 5(e)). Inspired by these works, a set of PSMAs (PF2-DTC, PF2-DTSi, and PF2-DTGe) (Fig. 1)[66] were developed to make mechanically robust all-PSCs. The all-PSCs based on PF2-DTSi achieved the highest PCE of 10.77% as well as a high toughness of 9.3 MJ/m^3 and an elongation at break of 8.6%. These studies clearly showed that all-PSCs have bright prospect for flexible and wearable applications.

In summary, new polymers made from isomerically pure monomers *via* simple and high-yield synthesis are required. PSMAs can be also synthesized by using non-fused ring small molecular acceptors. For conventional D–A type polymer acceptors, excellent device stability and mechanical properties

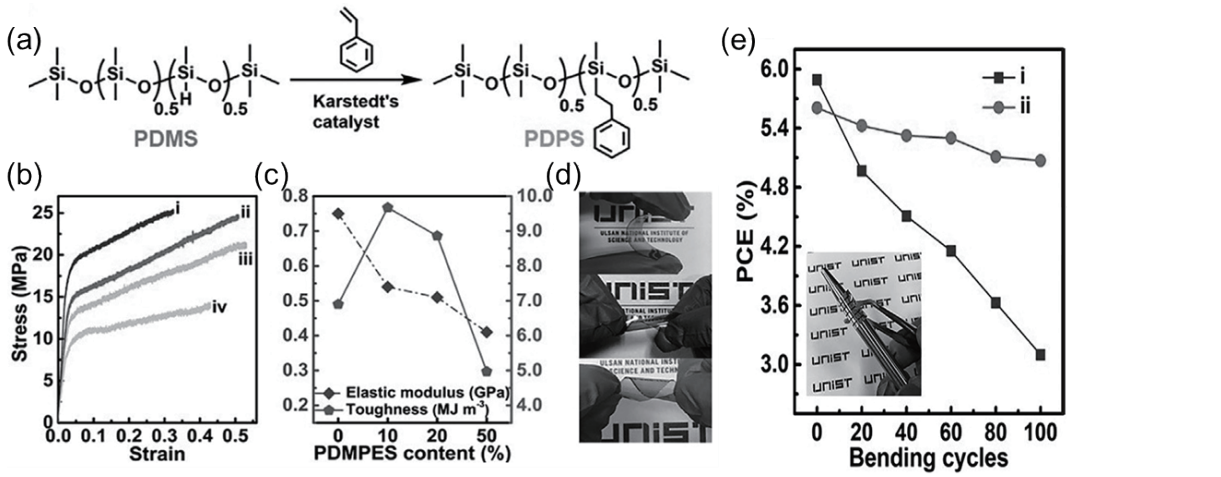

Fig. 5. (a) Synthetic route of PDPS. (b) The stress-strain curves and (c) corresponding elastic modulus and integrated toughness values for the blend films with different PDPS content. (i) 0PDPS (0% PDPS), (ii) 10PDPS (10% PDPS), (iii) 20PDPS (20% PDPS), (iv) 50PDPS (50% PDPS). (d) The different bending for the blend films on PET substrate. (e) PCEs for 0PDPS and 10PDPS based flexible all-PSCs (bending radius 3 mm). Reproduced with permission[65], Copyright 2018, John Wiley and Sons.

provide them unique advantages. These polymers will be practically useful provided that the PCE can be significantly enhanced. More efforts should be devoted to rational polymer design and morphology control. More morphology regulation strategies will greatly speed up the advances of all-PSCs.

Acknowledgements

This research was financially supported by the National Key Research and Development Program of China (2017YFA0206600), Guangdong Innovative and Entrepreneurial Research Team Program (2019ZT08L075), Open Funds of State Key Laboratory of Fine Chemicals (KF1901), and the Fundamental Research Funds for the Central Universities (D2190310). L. Ding appreciates the National Natural Science Foundation of China (51773045, 21772030, 51922032, 21961160720) for financial support.

References

[1] Liu Q, Jiang Y, Jin K, et al. 18% efficiency organic solar cells. Sci Bull, 2020, 65, 272
[2] Lin Y, Firdaus Y, Isikgor F H, et al. Self-assembled monolayer enables hole transport layer-free organic solar cells with 18% efficiency and improved operational stability. ACS Energy Lett, 2020, 5, 2935
[3] Lin Y, Nugraha M I, Firdaus Y, et al. A simple n-dopant derived from diquat boosts the efficiency of organic solar cells to 18.3%. ACS Energy Lett, 2020, 5, 3663
[4] Zhang M, Zhu L, Zhou G, et al. Single-layered organic photovoltaics with double cascading charge transport pathways: 18% efficiencies. Nat Commun, 2021, 12, 309
[5] Zhan L, Li S, Xia X, et al. Layer-by-layer processed ternary organic photovoltaics with efficiency over 18%. Adv Mater, 2021, 33, 2007231
[6] Lin Y, Magomedov A, Firdaus Y, et al. 18.4% organic solar cells using a high ionization energy self-assembled monolayer as hole extraction interlayer. ChemSusChem, 2021, in press
[7] Lee C, Lee S, Kim G U, et al. Recent advances, design guidelines, and prospects of all-polymer solar cells. Chem Rev, 2019, 119, 8028
[8] Sun R, Wang W, Yu H, et al. Achieving over 17% efficiency of ternary all-polymer solar cells with two well-compatible polymer acceptors. Joule, 2021, 5, 1548
[9] Liu T, Yang T, Ma R, et al. 16% efficiency all-polymer organic solar cells enabled by a finely tuned morphology via the design of ternary blend. Joule, 2021, 5, 914
[10] Ma R, Yu J, Liu T, et al. All-polymer solar cells with over 16% efficiency and enhanced stability enabled by compatible solvent and polymer additives. Aggregate, 2021, in press
[11] Jia T, Zhang J, Zhang K, et al. All-polymer solar cells with efficiency approaching 16% enabled using a dithieno[3',2': 3,4;2",3": 5,6]benzo[1,2c][1,2,5]thiadiazole (fDTBT)-based polymer donor. J Mater Chem A, 2021, 9, 8975
[12] Fu H, Li Y, Yu J, et al. High efficiency (15.8%) all-polymer solar cells enabled by a regioregular narrow bandgap polymer acceptor. J Am Chem Soc, 2021, 143, 2665
[13] Duan C, Ding L. The new era for organic solar cells: polymer acceptors. Sci Bull, 2020, 65, 1508
[14] Yang J, Xiao B, Tang A, et al. Aromatic-diimide-based n-type conjugated polymers for all-polymer solar cell applications. Adv Mater, 2019, 31, 1804699
[15] Genene Z, Mammo W, Wang E, et al. Recent advances in n-type polymers for all-polymer solar cells. Adv Mater, 2019, 31, 1807275
[16] Wang G, Melkonyan F S, Facchetti A, et al. All-polymer solar cells: recent progress, challenges, and prospects. Angew Chem Int Ed, 2019, 58, 4129
[17] Sun H, Wang L, Wang Y, et al. Imide-functionalized polymer semiconductors. Chem Eur J, 2019, 25, 87
[18] Shi Q, Wu J, Wu X, et al. Perylene diimide-based conjugated polymers for all-polymer solar cells. Chem Eur J, 2020, 26, 12510
[19] Gao L, Zhang Z G, Xue L, et al. All-polymer solar cells based on absorption-complementary polymer donor and acceptor with high power conversion efficiency of 8.27%. Adv Mater, 2016, 28, 1884
[20] Fan B, Ying L, Wang Z, et al. Optimisation of processing solvent and molecular weight for the production of green-solvent-processed all-polymer solar cells with a power conversion efficiency over 9%. Energy Environ Sci, 2017, 10, 1243
[21] Liu X, Zou Y, Wang H Q, et al. High-performance all-polymer solar cells with a high fill factor and a broad tolerance to the donor/acceptor ratio. ACS Appl Mater Interfaces, 2018, 10, 38302
[22] Zhu L, Zhong W, Qiu C, et al. Aggregation-induced multilength scaled morphology enabling 11.76% efficiency in all-polymer solar cells using printing fabrication. Adv Mater, 2019, 31, 1902899
[23] Yan H, Chen Z, Zheng Y, et al. A high-mobility electron-transporting polymer for printed transistors. Nature, 2009, 457, 679

[24] Lee J W, Sung M J, Kim D, et al. Naphthalene diimide-based terpolymers with controlled crystalline properties for producing high electron mobility and optimal blend morphology in all-polymer solar cells. Chem Mater, 2020, 32, 2572
[25] Wu Y, Schneider S, Walter C, et al. Fine-tuning semiconducting polymer self-aggregation and crystallinity enables optimal morphology and high-performance printed all-polymer solar cells. J Am Chem Soc, 2020, 142, 392
[26] Lee J W, Choi N, Kim D, et al. Side chain engineered naphthalene diimide-based terpolymer for efficient and mechanically robust all-polymer solar cells. Chem Mater, 2021, 33, 1070
[27] Tran D K, Kolhe N B, Hwang Y J, et al. Effects of a fluorinated donor polymer on the morphology, photophysics, and performance of all-polymer solar cells based on naphthalene diimide-arylene copolymer acceptors. ACS Appl Mater Interfaces, 2020, 12, 16490
[28] Li Z, Ying L, Zhu P, et al. A generic green solvent concept boosting the power conversion efficiency of all-polymer solar cells to 11%. Energy Environ Sci, 2019, 12, 157
[29] Liu X, Li X, Wang L, et al. Synergistic effects of the processing solvent and additive on the production of efficient all-polymer solar cells. Nanoscale, 2020, 12, 4945
[30] Seo S, Kim J, Kang H, et al. Polymer donors with temperature-insensitive, strong aggregation properties enabling additive-free, processing temperature-tolerant high-performance all-polymer solar cells. Macromolecules, 2020, 54, 53
[31] Xie B, Zhang K, Hu Z, et al. Polymer pre-aggregation enables optimal morphology and high performance in all-polymer solar cells. Sol RRL, 2019, 4, 1900385
[32] Zhang Y, Xu Y, Ford M J, et al. Thermally stable all-polymer solar cells with high tolerance on blend ratios. Adv Energy Mater, 2018, 8, 1800029
[33] Kim M, Kim H I, Ryu S U, et al. Improving the photovoltaic performance and mechanical stability of flexible all-polymer solar cells via tailoring intermolecular interactions. Chem Mater, 2019, 31, 5047
[34] Liu X, Zhang C, Duan C, et al. Morphology optimization via side chain engineering enables all-polymer solar cells with excellent fill factor and stability. J Am Chem Soc, 2018, 140, 8934
[35] Dou C, Ding Z, Zhang Z, et al. Developing conjugated polymers with high electron affinity by replacing a C-C unit with a B←N unit. Angew Chem Int Ed, 2015, 54, 3648
[36] Li Y, Meng H, Liu T, et al. 8.78% efficient all-polymer solar cells enabled by polymer acceptors based on a B←N embedded electron-deficient unit. Adv Mater, 2019, 31, 1904585
[37] Zhao R, Wang N, Yu Y, et al. Organoboron polymer for 10% efficiency all-polymer solar cells. Chem Mater, 2020, 32, 1308
[38] Shi S, Chen P, Chen Y, et al. A narrow-bandgap n-type polymer semiconductor enabling efficient all-polymer solar cells. Adv Mater, 2019, 31, 1905161
[39] Feng K, Huang J, Zhang X, et al. High-performance all-polymer solar cells enabled by n-type polymers with an ultranarrow bandgap down to 1.28 eV. Adv Mater, 2020, 32, 2001476
[40] Zhao R, Liu J, Wang L. Polymer acceptors containing B←N units for organic photovoltaics. Acc Chem Res, 2020, 53, 1557
[41] Xu X, Feng K, Yu L, et al. Highly efficient all-polymer solar cells enabled by p-doping of the polymer donor. ACS Energy Lett, 2020, 5, 2434
[42] Zhang Z G, Yang Y, Yao J, et al. Constructing a strongly absorbing low-bandgap polymer acceptor for high-performance all-polymer solar cells. Angew Chem Int Ed, 2017, 56, 13503
[43] Jia T, Zhang J, Zhong W, et al. 14.4% efficiency all-polymer solar cell with broad absorption and low energy loss enabled by a novel polymer acceptor. Nano Energy, 2020, 72, 104718
[44] Zhang Z G, Li Y. Polymerized small-molecule acceptors for high-performance all-polymer solar cells. Angew Chem Int Ed, 2021, 60, 4422
[45] Meng Y, Wu J, Guo X, et al. 11.2% efficiency all-polymer solar cells with high open-circuit voltage. Sci China Chem, 2019, 62, 845
[46] Peng F, An K, Zhong W, et al. A universal fluorinated polymer acceptor enables all-polymer solar cells with > 15% efficiency. ACS Energy Lett, 2020, 5, 3702
[47] Sun H, Yu H, Shi Y, et al. A narrow-bandgap n-type polymer with an acceptor-acceptor backbone enabling efficient all-polymer solar cells. Adv Mater, 2020, 32, 2004183
[48] Fan Q, An Q, Lin Y, et al. Over 14% efficiency all-polymer solar cells enabled by a low bandgap polymer acceptor with low energy loss and efficient charge separation. Energy Environ Sci, 2020, 13, 5017
[49] Su N, Ma R, Li G, et al. High-efficiency all-polymer solar cells with poly-small-molecule acceptors having π-extended units with broad near-IR absorption. ACS Energy Lett, 2021, 6, 728
[50] Wang H, Chen H, Xie W, et al. Configurational isomers induced significant difference in all-polymer solar cells. Adv Funct Mater, 2021, 31, 2100877
[51] Wang W, Wu Q, Sun R, et al. Controlling molecular mass of low-band-gap polymer acceptors for high-performance all-polymer solar cells. Joule, 2020, 4, 1070
[52] Zhang L, Jia T, Pan L, et al. 15.4% efficiency all-polymer solar cells. Sci China Chem, 2021, 64, 408
[53] Yu H, Qi Z, Yu J, et al. Fluorinated end group enables high-performance all-polymer solar cells with near-infrared absorption and enhanced device efficiency over 14%. Adv Energy Mater, 2020, 11, 2003171
[54] Wu Q, Wang W, Wu Y, et al. High-performance all-polymer solar cells with a pseudo-bilayer configuration enabled by a stepwise optimization strategy. Adv Funct Mater, 2021, 31, 2010411
[55] Yu H, Pan M, Sun R, et al. Regio-regular polymer acceptors enabled by determined fluorination on end groups for all-polymer solar cells with 15.2% efficiency. Angew Chem Int Ed, 2021, 60, 10137
[56] Luo Z, Liu T, Ma R, et al. Precisely controlling the position of bromine on the end group enables well-regular polymer acceptors for all-polymer solar cells with efficiencies over 15%. Adv Mater, 2020, 32, 2005942
[57] Zhu X, Hu L, Wang W, et al. Reversible chemical reactivity of nonfullerene acceptors for organic solar cells under acidic and basic environment. ACS Appl Energy Mater, 2019, 2, 7602
[58] Guo J, Wu Y, Sun R, et al. Suppressing photo-oxidation of nonfullerene acceptors and their blends in organic solar cells by exploring material design and employing friendly stabilizers. J Mater Chem A, 2019, 7, 25088
[59] Lv R, Geng S, Li S, et al. Influences of quinoid structures on stability and photovoltaic performance of nonfullerene acceptors. Sol RRL, 2020, 4, 2000286
[60] Liu H, Wang W, Zhou Y, et al. A ring-locking strategy to enhance the chemical and photochemical stability of A–D–A-type nonfullerene acceptors. J Mater Chem A, 2021, 9, 1080
[61] McNeill C R. Morphology of all-polymer solar cells. Energy Environ Sci, 2012, 5, 5653
[62] Xu Y, Yuan J, Liang S, et al. Simultaneously improved efficiency and stability in all-polymer solar cells by a P–i–N architecture. ACS Energy Lett, 2019, 4, 2277
[63] Li N, McCulloch I, Brabec C J. Analyzing the efficiency, stability and cost potential for fullerene-free organic photovoltaics in one figure of merit. Energy Environ Sci, 2018, 11, 1355
[64] Kim T, Kim J H, Kang T E, et al. Flexible, highly efficient all-polymer solar cells. Nat Commun, 2015, 6, 8547
[65] Chen S, Jung S, Cho H J, et al. Highly flexible and efficient all-polymer solar cells with high-viscosity processing polymer additive toward potential of stretchable devices. Angew Chem Int Ed, 2018, 57, 13277
[66] Fan Q, Su W, Chen S, et al. Mechanically robust all-polymer solar cells from narrow band gap acceptors with hetero-bridging atoms. Joule, 2020, 4, 658

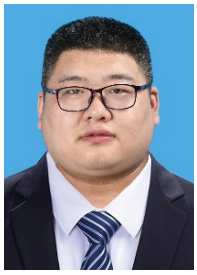

Baoqi Wu is currently a PhD candidate under the supervision of Prof. Chunhui Duan at South China University of Technology. He received his MS from Xiangtan University in 2018. His research focuses on polymer acceptors.

Bingyan Yin is currently a PhD candidate under the supervision of Prof. Chunhui Duan at South China University of Technology. She received her BS from South China University of Technology and MS from Sichuan University in 2017 and 2020, respectively. Her research focuses on organic solar cells and near-infrared organic photodetectors.

Chunhui Duan is a full professor in Department of Materials Science & Engineering, South China University of Technology. He received his BS from Dalian University of Technology in 2008 and PhD from South China University of Technology in 2013. After a postdoc training in Eindhoven University of Technology, he joined South China University of Technology in 2017. His research focuses on conjugated materials and their applications in optoelectronic devices including solar cells, photodetectors and transistors.

Liming Ding got his PhD from University of Science and Technology of China (was a joint student at Changchun Institute of Applied Chemistry, CAS). He started his research on OSCs and PLEDs in Olle Inganäs Lab in 1998. Later on, he worked at National Center for Polymer Research, Wright-Patterson Air Force Base and Argonne National Lab (USA). He joined Konarka as a Senior Scientist in 2008. In 2010, he joined National Center for Nanoscience and Technology as a full professor. His research focuses on innovative materials and devices. He is RSC Fellow, the nominator for Xplorer Prize, and the Associate Editors for Science Bulletin and Journal of Semiconductors.